ELSEVIER

Journal of Structural Geology 29 (2007) 863–880

JOURNAL OF STRUCTURAL GEOLOGY

www.elsevier.com/locate/jsg

Pre- to syn-extension melt-assisted nucleation and growth of extensional gneiss domes: The western French Massif Central (Variscan belt)

Jean-Philippe Bellot [a,b,*]

[a] *ISTEEM, Université Montpellier II, Place Eugène Bataillon, 34095 Montpellier Cedex 05, France*
[b] *BRGM, BP 6009, REM/MESY, 3 Avenue Claude Guillemin, 45060 Orléans Cedex 2, France*

Received 10 March 2006; received in revised form 28 December 2006; accepted 2 January 2007
Available online 18 January 2007

Abstract

Evidence for melt-assisted development of extensional gneiss domes is provided using the combined analysis of geological, geophysical, and geochronological data on the Millevaches dome and the adjacent Argentat fault (AF), in the western Massif Central, France. The Millevaches dome consists of mica-schists associated with monzogranites (344–342 Ma), migmatites (337–334 Ma) and leucogranites (329–318 Ma). These melts were emplaced before, at the onset of, and during the slip of the AF (~335–315 Ma), respectively. The AF is a 5-km-wide, crustal-scale, westward dipping shear zone along which S_3 foliation strikes NNW and L_3 lineation trends WNW. Kinematic indicators show uniform top-to-the WNW sense of shear coeval with retrograde low-pressure metamorphism, indicative of a normal-sense movement along the AF. The Millevaches dome is interpreted to be an extensional gneiss dome cored by migmatites and monzogranite derived from a mid-crustal molten layer inherited from collision and modified by addition of syn-extension leucogranites. The dome formed by crustal-scale normal shearing along the AF and coeval exhumation of deep-seated rocks in the footwall. Pre-extension melts have allowed dome nucleation at the onset of extension by localizing normal shearing within the molten layer. Syn-extension melts, given their quantity and emplacement mode within the dome, have enhanced the persistence of dome growth and its ultimate geometry.

Keywords: Extensional gneiss dome; Late-orogenic extension; Normal shear zone; Exhumation; Variscan belt

1. Introduction

Extensional gneiss domes, and their metamorphic core complex equivalents, are dome-shaped structures of high-grade metamorphosed rocks exhumed along a crustal-scale normal fault (i.e., detachment) in response to horizontal extension and subsequent erosion (e.g. Crittenden et al., 1980; Coney and Harms, 1984; Malavieille, 1993; Brun and Van Den Driessche, 1994; Vanderhaeghe and Teyssier, 2001). They result from the partitioning of extensional strain on one or more normal faults or shear zones, and their finite geometry reflects the interaction pattern of these faults (e.g. Wernicke and Axen, 1988; Buck, 1991; Brun et al., 1994; Gautier and Brun, 1994). In the hangingwall of the detachments, development of sedimentary basins reflects concurrent rotational normal faulting and erosion of the exhumed footwall. These two mechanisms are active over several million years (e.g. Dèzes et al., 1999; McClelland and Gilotti, 2003). Exhumation of deep-seated rocks in the footwall produces partial melting of fertile rocks (e.g. Brown, 1993; Thompson and Connolly, 1995) and LP-HT metamorphism (e.g. Thompson and Ridley, 1987) associated with granite emplacement (e.g. Burg et al., 1984; Guillot et al., 1994; Faure, 1995) and hydrothermal alteration (e.g. Smith et al., 1991).

The kinematics of extensional gneiss domes are mainly controlled by the genetic links and/or interactions between

* Present address: 4 Place de Brie, 13015 Marseille, France.
E-mail address: jpbellot@wanadoo.fr

0191-8141/$ - see front matter © 2007 Elsevier Ltd. All rights reserved.
doi:10.1016/j.jsg.2007.01.001

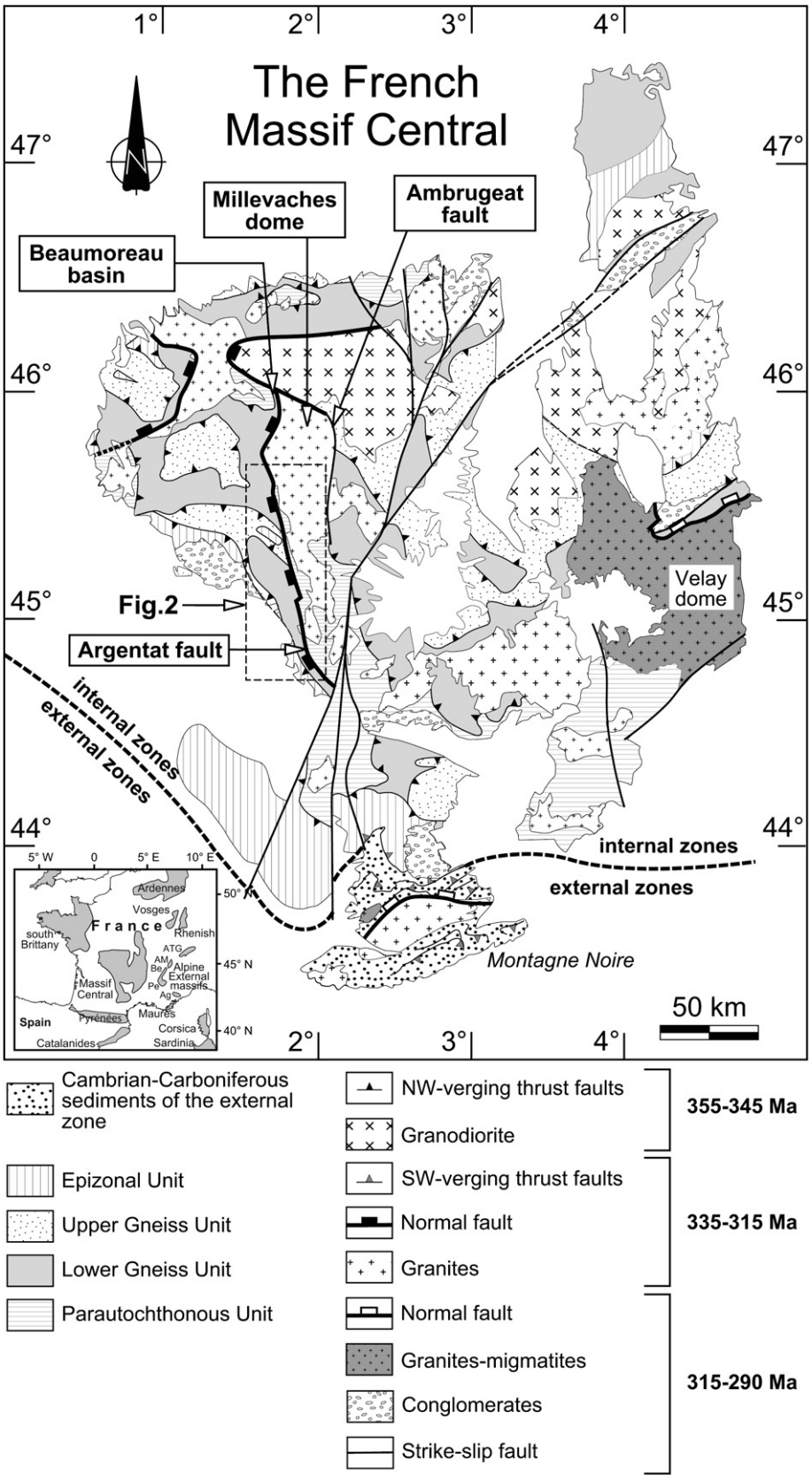

Fig. 1. Simplified map of the Massif Central with location of the Argentat fault, the Millevaches dome, and other structures of Late Palaeozoic age.

melting, plutonism and deformation within the dome and along the flanking detachment (Lister and Baldwin, 1993; Vanderhaeghe et al., 2003; Johnson, 2006). A key question is to know whether the shear zone controls magma emplacement or whether magma assists nucleation of the shear zone? The problem may be solved by studying the kinematics of normal-sense shear zones and the adjacent gneiss domes, and by determining the timing of melt generation and emplacement with respect to the development of the deformation pattern.

The aim of this paper is to use the results of a structural and kinematic study of ductile structures along the Argentat fault (AF) and the adjacent Millevaches dome (Massif Central, France) as the basis for a general model for the development of extensional gneiss domes. Structural data are combined with reflection seismic data and available geochronological constraints in order to evaluate the interactions between melt emplacement and the kinematics of nucleation and growth of the Millevaches dome in the context of late orogenic extension.

2. Geological framework and previous studies

2.1. Outline of the Variscan orogeny in the Massif Central

The South Limousin area belongs to the Variscan orogenic belt of western Europe (Fig. 1), which resulted from the Palaeozoic convergence and collision between two continents, Laurentia-Baltica and Gondwana, and numerous microplates including Armorica and Avalonia (e.g. Ziegler, 1989; Franke, 2000; Matte, 2001). Oceanic and subsequent continental subduction occurred during the Late Silurian-Devonian (e.g. Lardeaux et al., 2001). Continent–continent collision and associated crustal thickening occurred during the Devonian-Carboniferous and caused thrust and wrench tectonics (D_1 and D_2 phase) (Brun and Burg, 1982; Ledru et al., 1994; Matte, 2001).

Late orogenic extension is polyphase and diachronous through the Massif Central. NW-directed synorogenic extension (D_3 phase) was active during the Middle Carboniferous (Burg et al., 1994; Faure, 1995; Faure et al., 2002; Roig et al., 2002). It began in the northern Massif Central at ~335 Ma and propagated southward until ~315 Ma, coeval with southward-verging thrust tectonics in the southern Massif Central (Arnaud et al., 2004). Synorogenic extension resulted in both granite emplacement and normal/strike-slip faulting. N- to NE-directed postorogenic extension (D_4 phase) occurred during the Late Carboniferous (310–290 Ma) and affected the entire Massif Central (Burg et al., 1994; Faure, 1995). In the eastern Massif Central, this event resulted in crustal-scale normal faulting, emplacement of the granite-migmatite Velay dome (Fig. 1), and deposition of coal-bearing conglomerates in half graben-type basins (Echtler and Malavieille, 1990; Malavieille et al., 1990; Brun and Van Den Driessche, 1994; Ledru et al., 2001). In the western Massif Central, postorogenic extension accompanied wrench reactivation of preexisting faults along which coarse clastic sedimentation took place (Faure, 1995; Bellot et al., 2005).

2.2. Geological framework of the South Limousin area

2.2.1. The Limousin units

The upper crust of the South Limousin area (Fig. 2A) consists of four units. These are, in order from top to bottom: (a) the Epizonal Unit, made of schists, quartzites, and metabasites, (b) the Upper Gneiss Unit, that consists of eclogite boudins hosted by paragneiss, (c) the Lower Gneiss Unit, made of Cambrian-Ordovician orthogneiss intruding Precambrian paragneiss and mica-schist, (d) the Parautochthonous Unit, composed of quartzites and mica-schists and mapped along the western boundary of the Millevaches dome (Guillot, 1981; Floc'h, 1983). Stacking of these units is a consequence of Early Carboniferous (~355 Ma) NW-verging thrust tectonics (D_2 phase), associated with the development of S_{1-2} regional foliation, F_2 sheath folds and L_2 stretching lineation (Floc'h, 1983; Bouchez and Jover, 1986; Ledru et al., 1994; Roig and Faure, 2000; Bellot, 2004). Inverted Barrovian-type metamorphism also resulted from pilling of these units (Guillot, 1981; Floc'h, 1983; Bellot, 2001). Late stages of the D_2 phase (355–345 Ma) caused transcurrent tectonics involving ductile sinistral strike-slip shearing (Estivaux shear zone), early regional-scale folding (Uzerche synform, Tulle and Meuzac antiforms), and granodiorite emplacement (Roig et al., 1996, 1998) (Fig. 2).

2.2.2. The Argentat fault

The AF juxtaposes the Limousin metamorphic units, in the west, and the Millevaches granite, in the east (Fig. 1) (Mouret, 1922; Floc'h, 1983; Feix, 1988; Ledru et al., 1994; Roig et al., 2002). The trace of the AF, which trends 165°E, is 180 km long. This fault is suspected to have experienced a normal motion in relation to NW-SE extension (Mattauer et al., 1988; Ledru et al., 1994; Roig et al., 2002). Hydrothermal muscovites sampled along the AF yielded ^{40}Ar-^{39}Ar ages of 335 ± 4 Ma and 337 ± 4 Ma (Fig. 2A) (Roig et al., 2002). Fireclays from the lowermost part of the sedimentary sequence of the Beaumoreau basin (Fig. 1) occurring in the easternmost part of the hangingwall of the AF have yielded a zircon U-Pb age of 332 ± 4 Ma (Bruguier et al., 1998). These data suggest that channelling of hydrothermal fluid occurred along the AF during normal shearing, in the Upper Visean (337–332 Ma).

2.2.3. The Millevaches dome

The Millevaches dome consists of mica-schists of the Parautochthonous Unit intruded by several generations of granite associated with migmatites and granulites (Figs. 2A and 4A). The dome is bounded to the west by the AF and to the east by the Ambrugeat fault (Fig. 1). It is divided into two parts by the NNW-striking dextral Pradines shear zone (Mezure, 1981) (Fig. 1). In the western part of the dome, whole rock Rb-Sr dating has yielded an age of 467 ± 8 Ma for the orthogneiss protolith of the migmatites and 344 ± 8 Ma for the monzogranites (Monier, 1980). Monazite Th-U-Pb dating

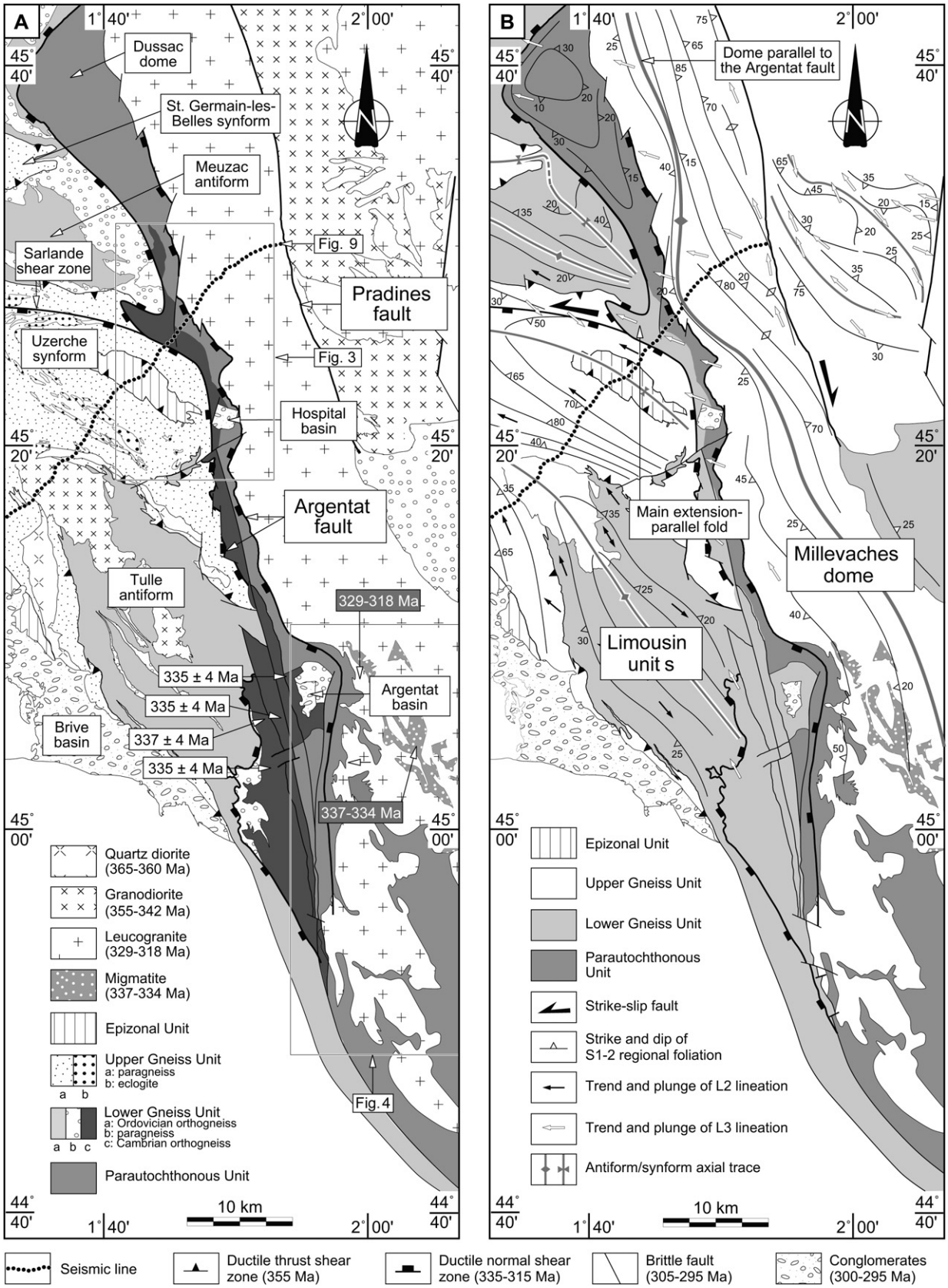

Fig. 2. Setting of the Argentat fault in the southwestern Massif Central (location in Fig. 1). (A) Geology. (B) Structure. Radiometric ages: in dark ^{40}Ar-^{39}Ar on muscovite, in white: Rb-Sr on whole-rock.

has yielded 342 ± 5 Ma for the monzogranites, 337 ± 4 Ma and 334 ± 4 Ma for the migmatites (Be Mézème, 2005), and 329 ± 8 Ma, 324 ± 3 Ma, 323 ± 4 Ma, and 318 ± 3 Ma for the leucogranites affected by the AF (Gébelin, 2004; Be Mézème, 2005; Fig. 4A). Therefore, melt generation and emplacement took place between 345 and 315 Ma in the western Millevaches dome, with the monzogranites forming first during collision (344–342 Ma), then the migmatites at the onset of extension (337–334 Ma), and finally the leucogranites during synorogenic extension (329–318 Ma). Along the Pradines shear zone, muscovite $^{40}Ar/^{39}Ar$ and monazite Th-U-Pb and U-Pb dating have yielded a common age of ~315 Ma for sheared leucogranites and for granulites paleosomes and neosomes (Gébelin, 2004), indicating that solid-state deformation of leucogranites and granulite metamorphism occurred coevally in relation to dextral movement of the Pradines shear zone during the latest stages of synorogenic extension (~315 Ma), as synorogenic extension is inferred to have lasted from 335 to 315 Ma (Faure, 1995).

The origin of the Millevaches granite is a matter of debate. Several hypothesis have been proposed:

- For Floc'h (1983) and Bouchez and Jover (1986), the Millevaches granite is syntectonic and was emplaced along a NW-verging thrust fault. This interpretation is in disagreement with (1) the time span of leucogranite emplacement (329–318 Ma) that coincides with the period of synorogenic extension dated 335–315 Ma in the internal zones of the Variscan belt (e.g. Faure et al., 2002), and (2) the close association of the Millevaches leucogranites with the AF, which itself crosscuts NW-verging thrusts (Floc'h, 1983; Roig and Faure, 2000; Bellot, 2004).
- According to Faure (1995), the granite is a laccolite that was emplaced in the core of a regional-scale antiform formed during synorogenic extension. However, this model does not explain the NNW-SSE orientation of an upright fold in the area, neither parallel nor perpendicular to the regional lineation.
- For Gébelin (2004) and Gébelin et al. (2006), the Millevaches granite would be a thin laccolite emplaced into a lithospheric-scale pop-up structure centred on the Pradines shear zone, and formed during "a strike-slip event rather than a late-orogenic extensional event". This model, supported by AMS investigations on the central part of the Millevaches, has two main inconsistencies. First, the rooting of the shear zone in the lower curst is not supported by any data. Second, the fact that "no significant imprint of Variscan extension is recognised in the internal fabric of the granite than the dextral motion of the Pradines shear zone" is surprising considering the span time of granite emplacement (345–315 Ma) that ranges from collision (355–345 Ma) to synorogenic extension (335–315 Ma).

Here we present new data on the Millevaches granite and the adjacent Argentat fault that provide a new model that integrates more satisfactorily the whole geological data set, and more particularly the geochronology of the various intrusions and the respective role of the AF and Pradines shear zone in generating the Millevaches dome and its internal granites.

3. Foliation and lineation pattern

3.1. Foliation pattern

At the regional scale, the AF is a major structural boundary that juxtaposes NW-SE-trending upright folds of the S_{1-2} foliation in the Limousin units, and an asymmetric gneiss dome (i.e. the Millevaches dome) delineated by the S_{1-2} foliation parallel to the AF in the Millevaches granite (Fig. 2B). Within the Limousin units, the hinge of the Uzerche synform exhibits pervasive NW-SE-trending conic folds of the S_{1-2} regional foliation, indicative of disharmonic folding (Fig. 3A). The AF is associated with intense reworking of the S_2–L_2 fabrics of the Limousin units and development of S_3–L_3 fabric in the Millevaches granite.

In orthogneisses of the western part of the dome, the S_{1-2} foliation strikes WNW-ESE and dips steeply or gently to the SSW, defining km-scale F_3 folds trending WNW-ESE and plunging gently to moderately to the WNW (Fig. 3A). Intense folding occurs between hinges of the Meuzac antiform and the Uzerche synform (Figs. 2B and 3A) and coincides with the eastern tip of the Sarlande sinistral-normal shear zone that dips moderately to the south and that formed by WNW-ESE-trending extension (Bellot, 2001) (Fig. 3A). Intense folding likely reflects interference between normal shearing along the AF and upright folding and normal-sinistral shearing in the Limousin units.

In mica-schists of the western part of the dome, the S_{1-2} foliation strikes NNW-SSE and dips either moderately to the west or gently to the east, defining F_3 folds parallel to the AF (Fig. 3A).

In the granites of the western part of the dome, the S_3 solid-state foliation strikes N-S to NNE-SSW and dips gently to moderately to the W/WSW. To the east, this foliation is involved in km-scale domes elongated and aligned parallel to the AF (Fig. 3A). In this zone, the leucogranites exhibit a shallowly-dipping to flat-lying, late magmatic to solid-state, S_3 foliation (Fig. 3C). These observations preclude the Millevaches granite as forming a single upright fold flanking the AF.

The structural pattern described above differs from that observed further to the south where the relations between the migmatites, monzogranites, leucogranites, and granodiorites of the footwall of the AF are better documented (Fig. 4A). Granodiorites and leucogranites (329–318 Ma) postdate migmatites (337–334 Ma) and monzogranites (344–342 Ma). Migmatites and monzogranites are spatially linked and are both involved in a dome elongated parallel to the AF (Fig. 4B). Monzogranites display a late magmatic to solid-state vertical foliation that strikes N150°E (Labernardière, 1992). Leucogranites and their host mica-schists display NNE-striking foliation with westward or eastward dip, defining F_3 folds parallel to the AF. Foliation deflects asymmetrically on both sides of granodiorite plutons to form triple points (c, d; e, f; g in Fig. 4B),

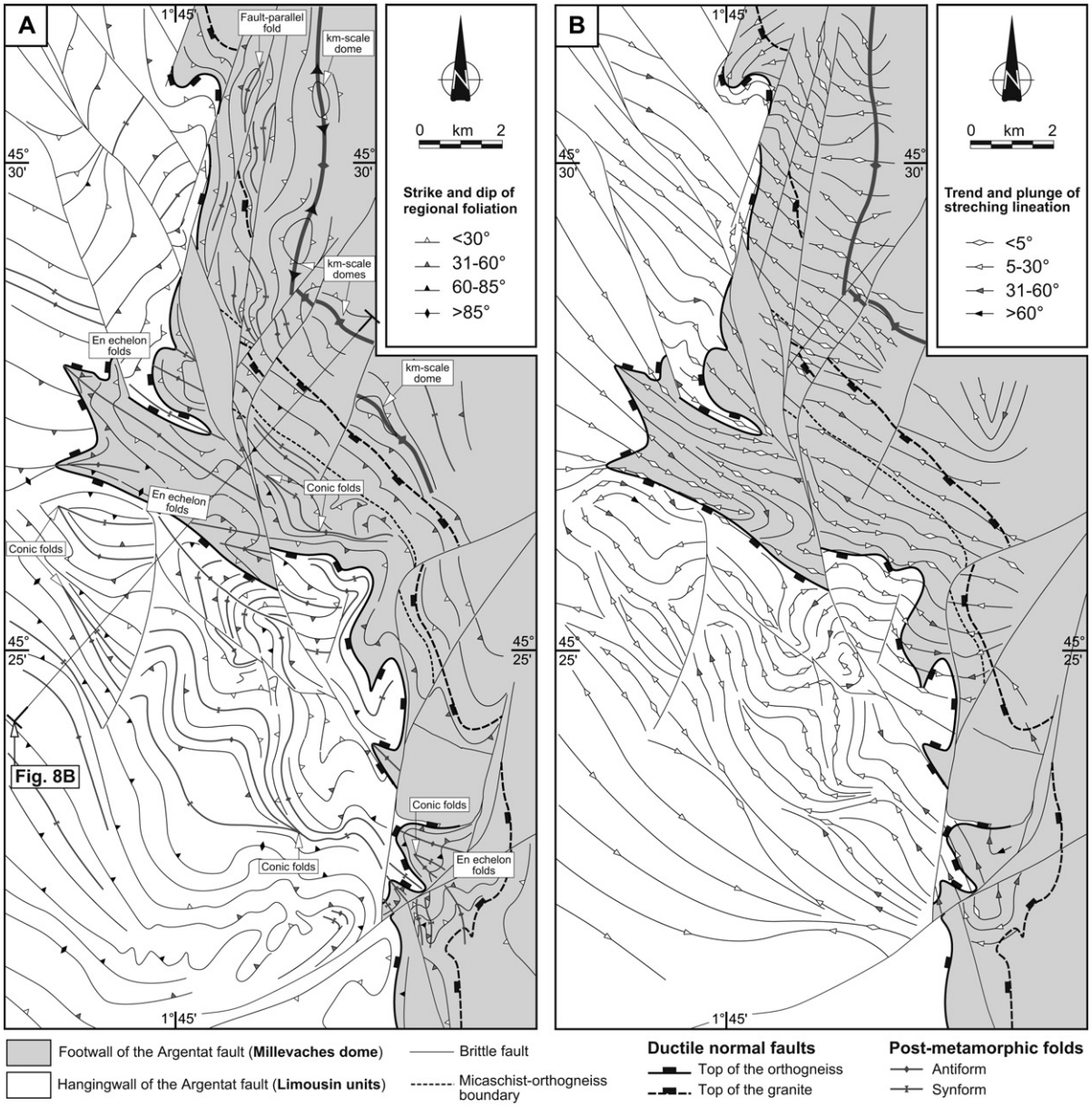

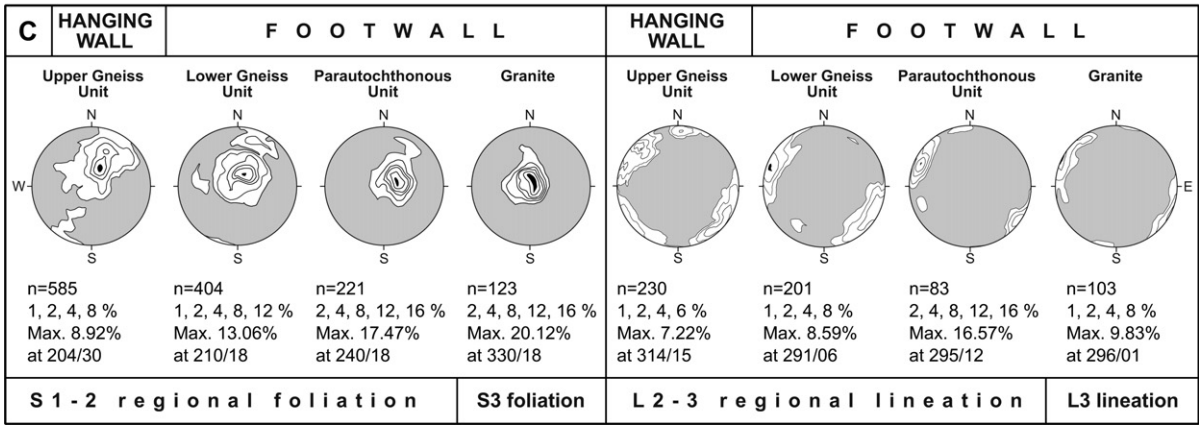

Fig. 3. Detailed structural maps of the Argentat fault in the western Millevaches dome (location in Fig. 2A). (A) Pattern of S_{1-2} foliation in metamorphic rocks and solid-state S_3 foliation in granite. (B) Pattern of L_{2-3} lineation in metamorphic rocks and solid-state L_3 lineation in granite. (C) Lower hemisphere, equal area, stereograms of structural data.

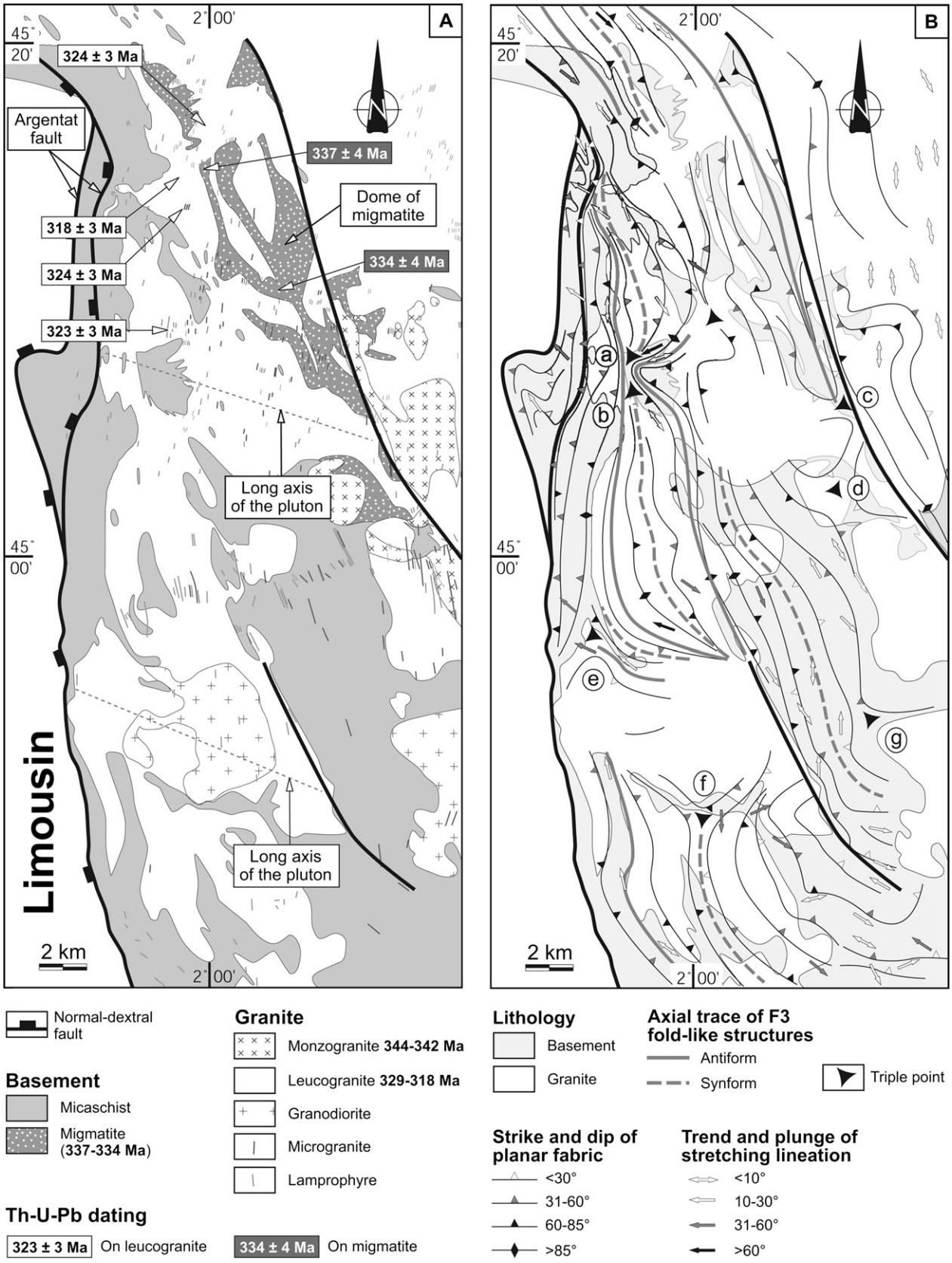

Fig. 4. Maps of the southwestern Millevaches dome (location in Fig. 2A). (A) Lithology. (B) Structure with pattern of S_{1-2} foliation in metamorphic rocks and solid-state S_3 foliation in granite.

indicative of a dextral component of shearing within the Millevaches dome. The granodiorite intruded to form WNW-ESE-elongated plutons (Fig. 4A). Their echelon pattern suggests WNW-ESE opening and plutonism within the Millevaches dome concomitant with a dextral component of shearing along the AF. These structures fit into a transtensional (dextral) kinematic framework along the AF. The mutually cross-cutting relationships between granodiorites and leucogranites suggest their coeval emplacement.

3.2. Lineation pattern

In the Limousin units, the L_3 lineation trends NW-SE and plunges gently to the SE. In the whole footwall of the AF, the L_3 lineation trends consistently WNW-ESE and plunges gently to the WNW (Fig. 3B).

In orthogneisses of the western part of the dome, S_3 and L_3 are re-folded by WNW-ESE-trending F_3 folds, as a consequence of progressive D_3 deformation. In mica-schists of the western part of the dome, L_3 direction does not vary on both limbs of WNW-ESE-trending F_3 folds and fault-parallel F_3 folds, suggesting these two groups of folds are coeval. In the leucogranites of the western part of the dome, L_3 lineations converge symmetrically toward second-order domes of S_3 foliation and diverges between them (Fig. 3B). In the southern Millevaches dome (Fig. 4B), the L_3 lineation trends consistently WNW-ESE and plunges gently to the WNW in zones of intense folding in the vicinity of the AF. Further to the east, the L_3 lineation trends NNW-SSE, parallel to the AF trend.

In incompetent rocks of both the hangingwall and footwall of the AF, patterns of S_{1-2} foliation, S_3 foliation (Fig. 3A), L_3 lineation (Fig. 3B), and F_3 folds (Fig. 3A) are gently refolded by F_4 folds in the vicinity of late brittle faults related to the D_4 tectonic event (Bellot et al., 2005).

4. Kinematics and metamorphism

Local field observations in the Limousin units are indicative of top-to-the WNW shearing along the AF: (1) along the western limb of the Dussac dome (Fig. 2A), asymmetric quartz-sillimanite-bearing nodules (Mouthier, 1976), (2) east of the Argentat basin (Fig. 2A), F_3 drag folds with fault-parallel horizontal axis and horizontal axial plane in mica-schists (Roig et al., 2002), (3) east of the Argentat basin, westward

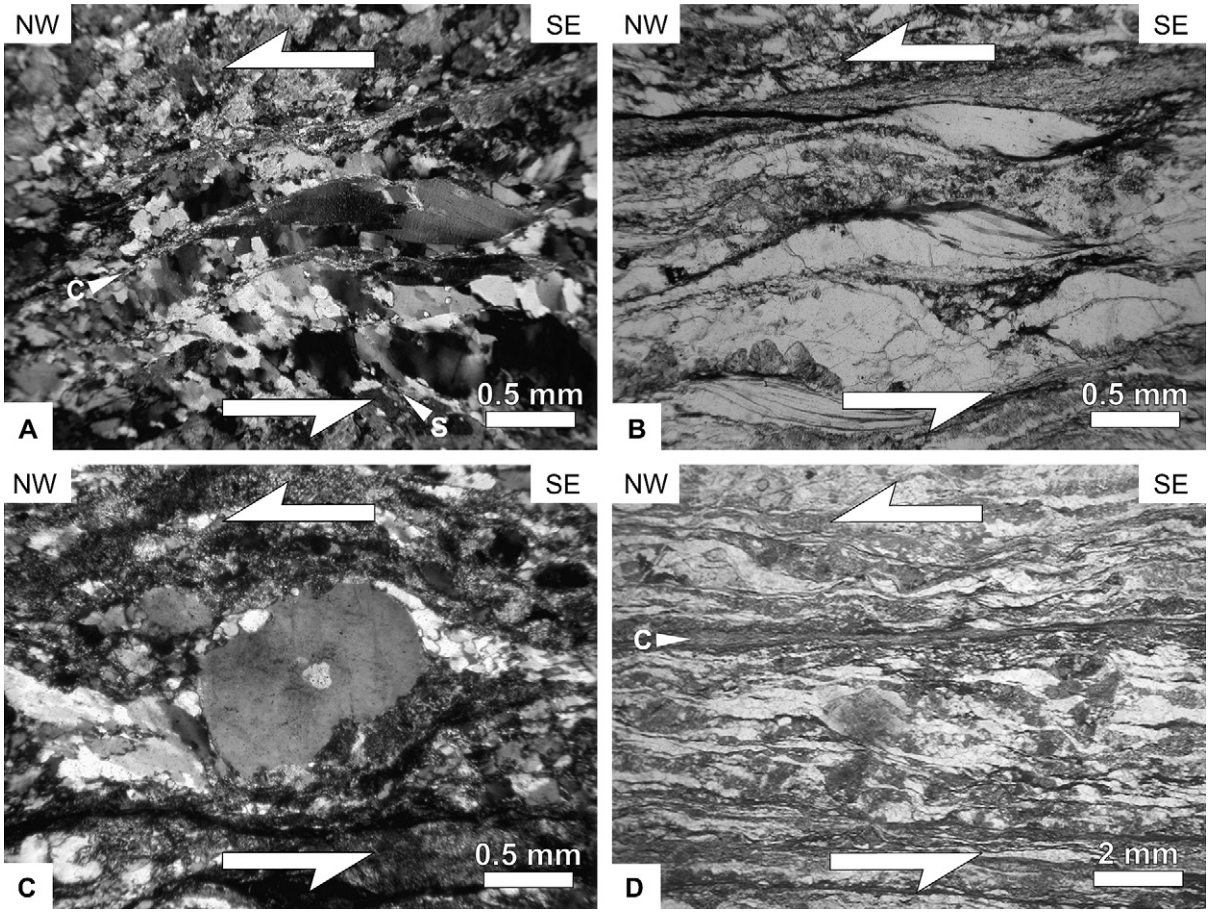

Fig. 5. Photomicrographs of key asymmetric structures observed in mylonitic orthogneiss along the AF, indicating a normal-dextral movement. (A) Preferred orientation of under-grain quartz defining a new foliation (S) oblique to the shear plane (C). (B) Fish-like muscovite, sigma-shaped quartz and quartz-feldspar aggregates. (C) Delta-type porphyroclast of quartz with asymmetric strain-shadows of recrystallised quartz. (D) Shear bands (C), sigma-shaped quartz, and quartz-feldspar aggregates.

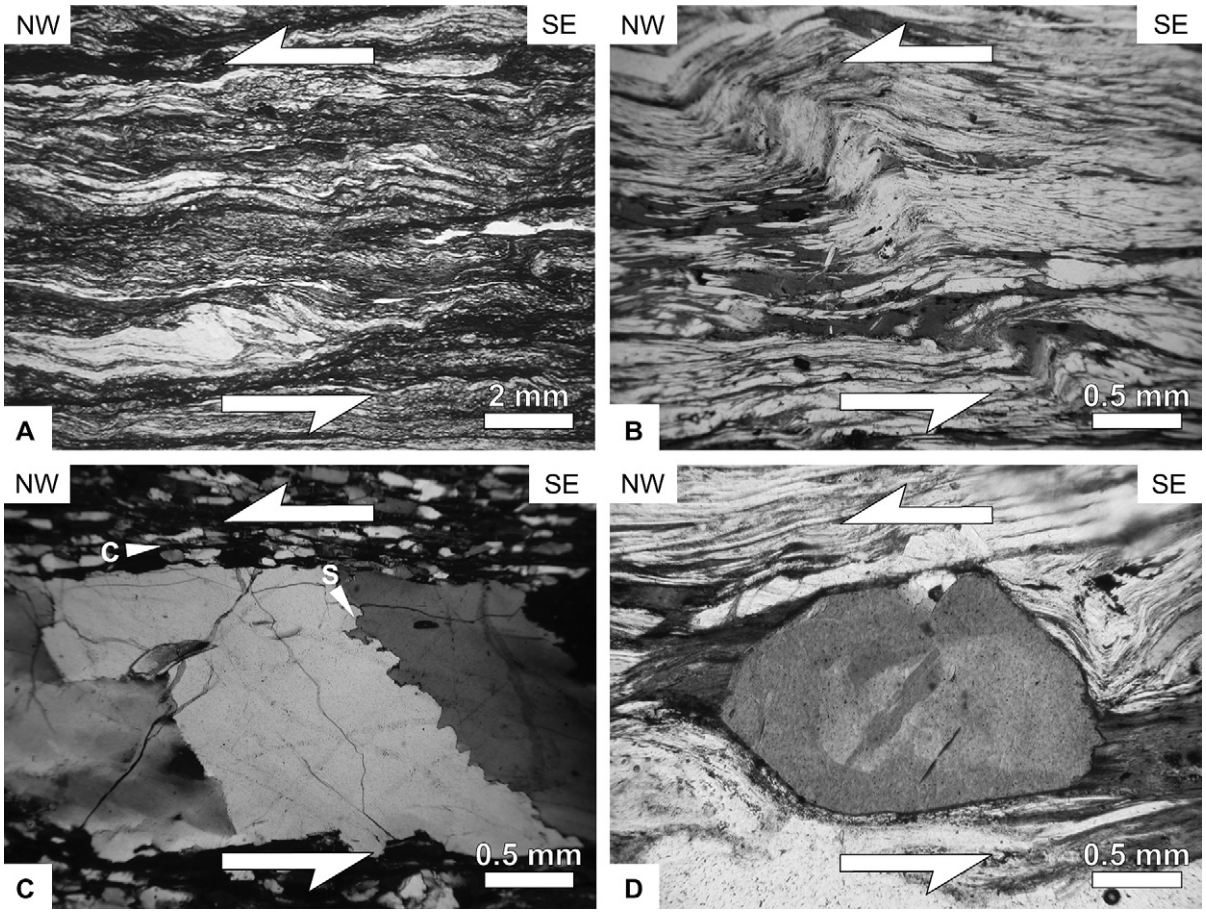

Fig. 6. Photomicrographs of key asymmetric structures observed in mylonitic mica-schist along the AF, indicating a normal-dextral movement. (A) Shear bands. (B) Post-metamorphic drag fold growing upward. (C) Quartz ribbon with preferred orientation of under-grain defining a new foliation (S) oblique to the shear plane (C). (D) Asymmetric tourmaline with asymmetric strain-shadows of biotite.

dipping C-planes in leucogranite (Roig et al., 2002). In order to confirm these results at a regional scale, an analysis of microstructures has been undertaken on 200 thin-sections cut normal to the S_3 foliation and parallel to the L_3 lineation, and sampled along the western and eastern sides of the Millevaches dome, close to the AF and the Ambrugeat fault, respectively.

4.1. Microstructures

Observed microstructures are usually asymmetric, indicating non-coaxial deformation within the AF.

In orthogneisses of the western part of the dome, asymmetric microstructures include the preferred orientation of sub-grain quartz defining a foliation oblique to the shear plane (Fig. 5A), fish-like muscovite (Fig. 5B), delta-type quartz porphyroclasts with asymmetric strain-shadows of recrystallised quartz (Fig. 5C), and sigma-shaped quartz or quartz-feldspar aggregates (Fig. 5D).

In mica-schists of the western part of the dome, asymmetric microstructures are shear bands (Fig. 6A), post-metamorphic drag folds (Fig. 6B), quartz ribbon with preferred orientation of sub-grains defining a foliation oblique to the shear plane (Fig. 6C), and asymmetric tourmaline crystals with asymmetric strain-shadows of biotite (Fig. 6D).

In the leucogranites of the western part of the dome, asymmetric microstructures are sigmoid-shaped muscovites (Fig. 7A) and feldspars with asymmetric strain shadows of dynamically recrystallised quartz (Fig. 7B). Frequent asymmetric-shaped magmatic textures indicate that granite emplacement and top-to-the NW shear deformation were coeval along the AF (Roig et al., 2002).

In the eastern part of the dome, close to the Ambrugeat fault (Fig. 1), leucogranites are deformed by a low-angle, westward dipping shear zone that exhibits late magmatic to solid-state asymmetric microstructures. These include shear bands (Fig. 7C), muscovite fish (Fig. 7D), asymmetric tails on feldspar grains (Fig. 7E), and preferred orientation of sub-grain quartz defining a foliation oblique to the shear plane (Fig. 7F).

To summarize, syn-D_3 top-to-the WNW shearing is inferred along the AF and within the Millevaches dome. There is no reversal of shear sense on opposite sides of the Millevaches dome, and on both sides of second-order domes within the Millevaches dome either. Normal-sense of shear prevailed along the AF during emplacement of the granites within the Millevaches dome.

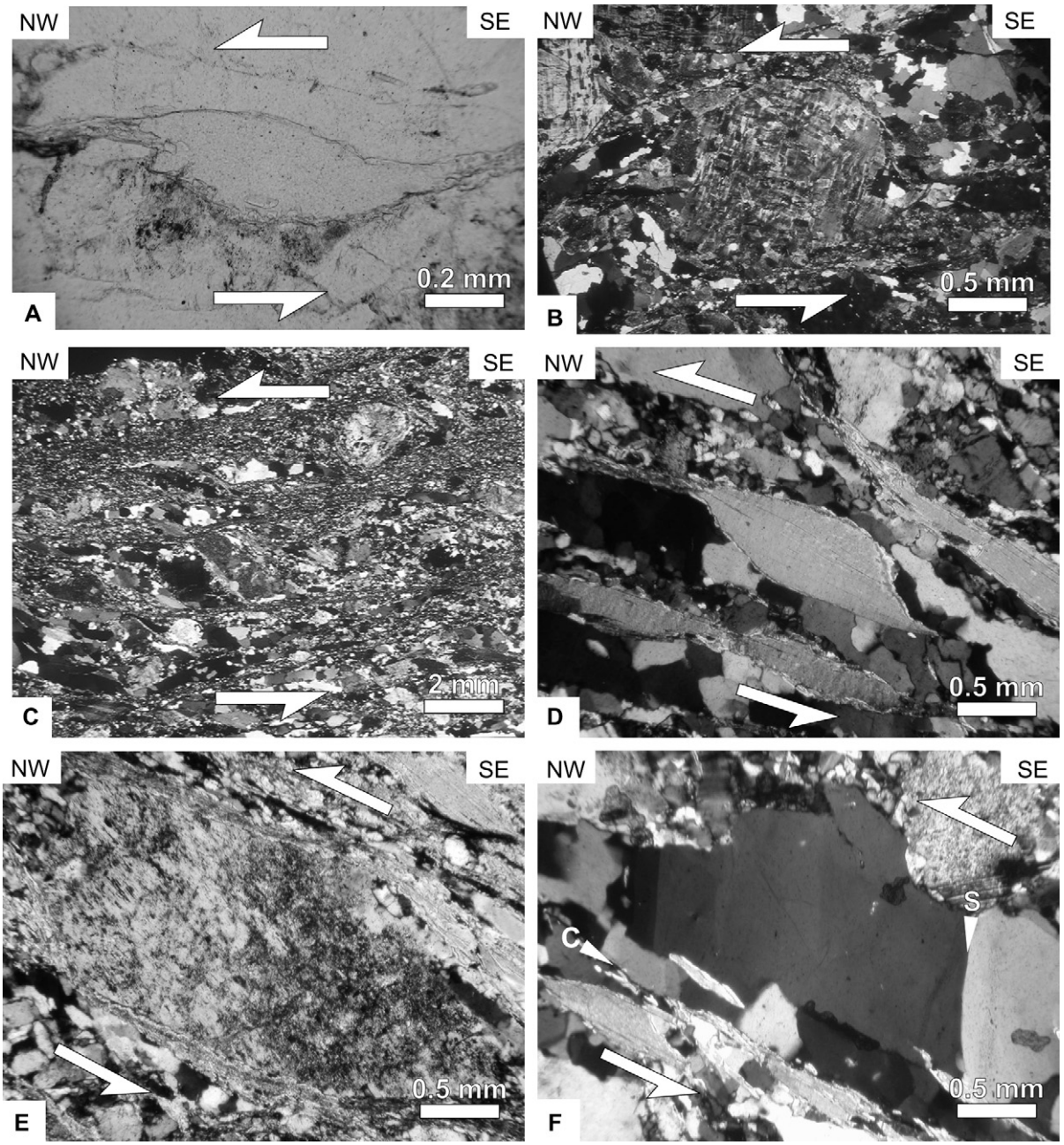

Fig. 7. Photomicrographs of key asymmetric structures observed in sheared leucogranite sited along the AF (A,B) or on the eastern margin of the Millevaches dome (C–F), indicating normal-dextral and normal movements, respectively. (A) Sigmoid-like shaped muscovite. (B) Feldspar with asymmetric strain shadows of dynamically recrystallised quartz. (C) Shear bands. (D) Fish-like shaped muscovite. (E) Asymmetric feldspar with asymmetric strain-shadows of recrystallised quartz. (F) Preferred orientation of under-grain quartz defining a new foliation (S) oblique to the shear plane (C).

4.2. Relationships between shear deformation and metamorphism

At a regional scale, syn-D_3 regional metamorphism in the Millevaches dome is attested by the parallelism between metamorphic zones and the trace of the AF, from chlorite in orthogneiss, to andalusite-biotite in mica-schist, and K-feldspar-sillimanite and cordierite in the granite-migmatite dome (Fig. 8A). In each metamorphic zone, mineral assemblages that grew during D_3 top-to-the WNW shearing indicate a succession of retrograde reactions in the KFMASH system (e.g. Spear et al., 1999).

P-T paths derived from observed reactions combined with thermobarometry (Bellot, 2001) indicate syn-D_3 decompression and heating, then decompression and cooling (Fig. 8A). Syn-D_3 heating increases toward the interior of the dome at intermediate pressure (0.45 GPa) from 550 to 650 °C. This may reflect partial melting (production of migmatite) and/or intrusion of melts near the roof of the Parautochthonous Unit at the onset of extension. Syn-D_3 cooling increases from the interior towards the western margin of the dome at low pressure (0.20 GPa) from 600 to 350 °C. This suggests syntectonic channelling of fluids within shears related to the AF.

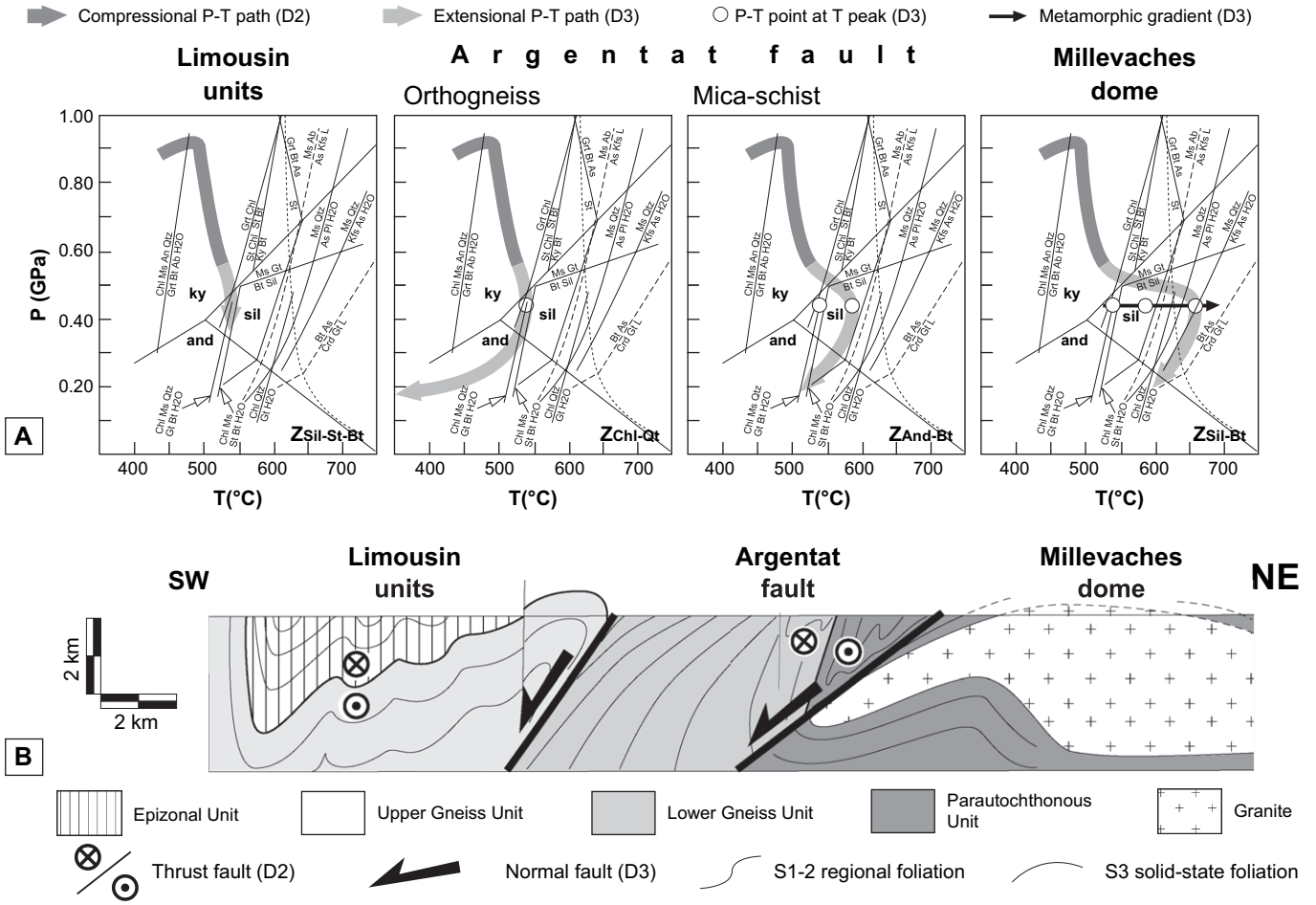

Fig. 8. (A) P-T paths obtained within metamorphic zones of the Argentat fault (adapted from Bellot, 2001) (location in Fig. 2). (B) Detailed geological cross-section parallel and along the seismic line (located in Fig. 3A).

Accordingly, syn-D_3 retrograde metamorphism in the Millevaches dome indicates that exhumation of deep-seated rocks and melt emplacement occurred contemporaneously during normal shearing along the AF.

5. Crustal geometry of Argentat fault and Millevaches dome

Contrasting foliation and lineation pattern, and microstructures indicate that the AF is a major boundary between Limousin units and the Millevaches dome. A recent reflection-seismic line perpendicular to the AF (Bitri et al., 1999) is used here to provide a new crustal-scale interpretation of the AF and the Millevaches dome (Figs. 9A–C and 10).

The zone of highest strain observed at the surface (i.e., the AF), occurs at the top of the mylonitic orthogneiss. This zone coincides with a major discontinuity that dips consistently 35° to the SW up to a depth of 15 km and that flattens to subhorizontal between 15 and 16 km depth (Fig. 9B). This discontinuity marks the boundary between a low-reflectivity crustal unit to the SW (hangingwall) and a moderately reflective block to the NE (footwall). In the footwall, at a depth of 7–14 km, the flat-lying seismic fabric is crosscut by three discontinuities dipping parallel to the main discontinuity and connecting downward to the latter at ~18 km depth. The westernmost of these discontinuities coincides at the surface with the shear zone located at the mica-schist-granite boundary (Fig. 3A). The two other discontinuities likely link upwards and terminate at 8 km depth. These discontinuities may be thrust faults. However, NE-verging thrusts are unknown in the region (Ledru et al., 1994). These discontinuities are therefore interpreted to form secondary shear zones of a crustal-scale Argentat shear system. The reverse movement observed in the SW-NE section may be considered as apparent and due to shortening normal to the extension direction. In the footwall of the AF, at 4–8 km depth, the seismic fabric underlines a 10-km-wide dome that suggests fabric deflection toward the SW, suggesting that the Millevaches dome is a crustal-scale structure. At the northeastern boundary of the seismic profile, at a depth of 8–15 km, a vertical discontinuity crosscuts flat reflectors. This discontinuity coincides at the surface with the Pradines dextral shear zone. The Pradines shear zone appears to be restricted to the upper-middle crust and does not crosscut the lower crust.

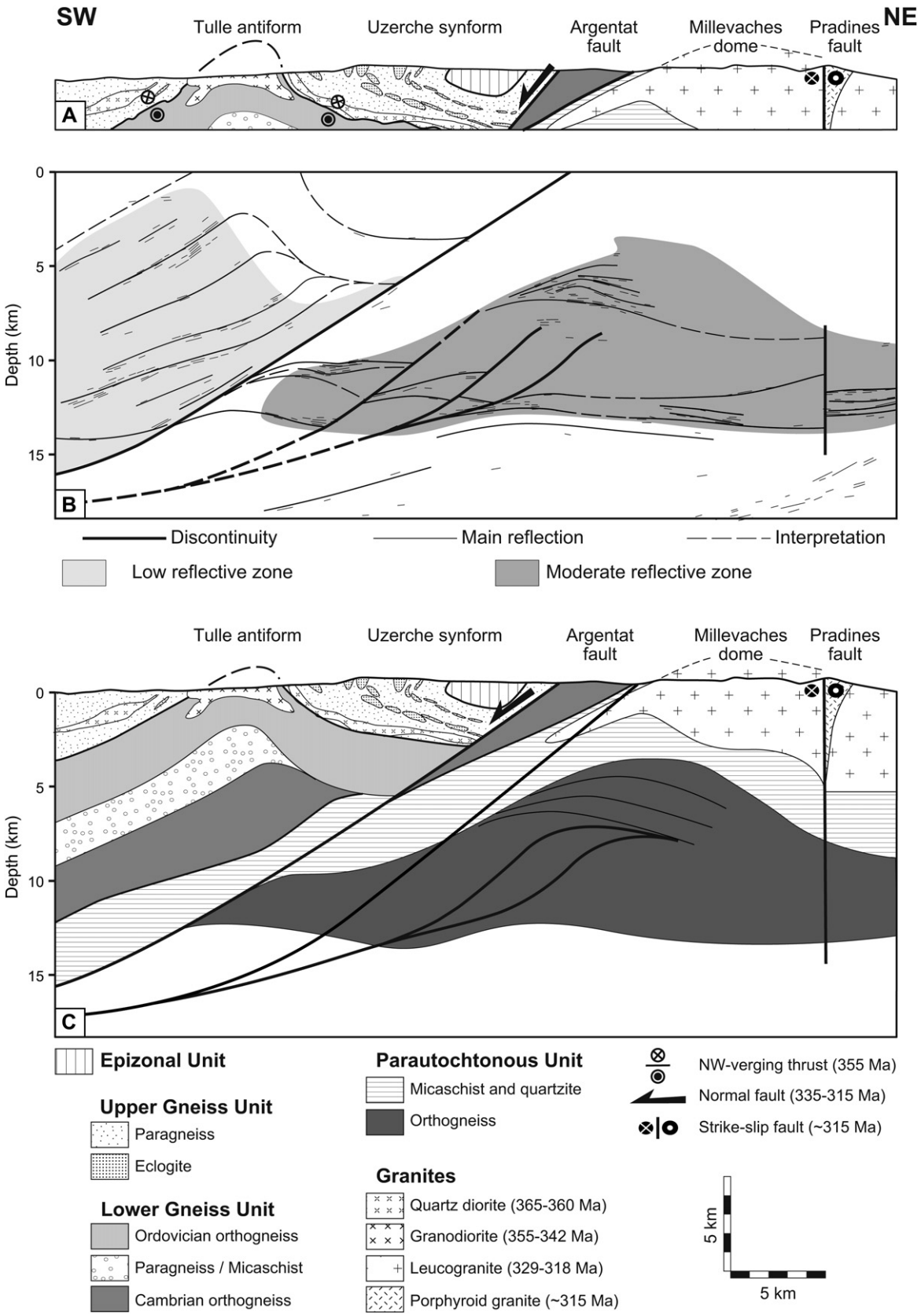

Fig. 9. Vertical seismic section throughout the Argentat fault. (A) Geological cross-section parallel to and along the seismic line, drawn from surface data. (B) Simplified line drawing (location in Fig. 2). (C) Geological interpretation of (B). The parameters of seismic acquisition were previously reported by Bitri et al. (1999).

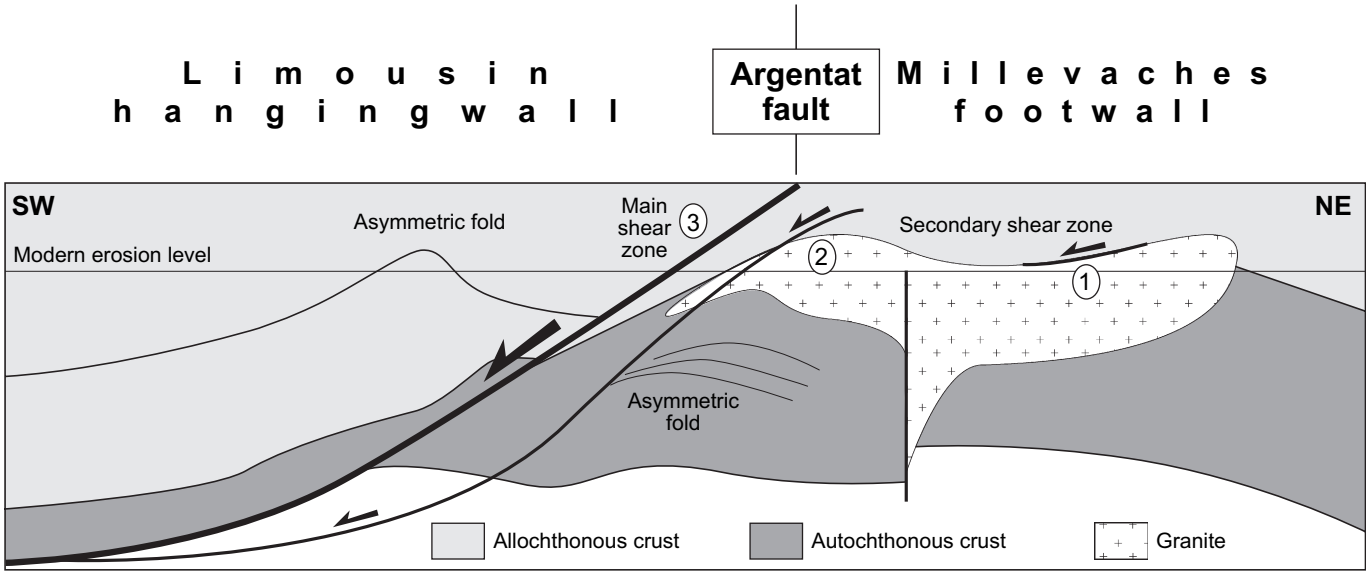

Fig. 10. Synthetic cross-section though the Argentat fault and the Millevaches dome. Numbers 1, 2 and 3 indicate the possible sequence of development of shear zones of the Argentat fault system.

6. Shear strain and displacement along the shear zone

Within the Millevaches dome, shear deformation is penetrative in orthogneisses, moderate in the mica-schists, and weak in the granites-migmatites. This suggests that strain increases gradually towards the AF. In order to quantify this gradient, a quantitative estimate of shear strain and corresponding displacement has been performed: (1) within these three lithological units, from thin sections study; and (2) for the whole AF, using the crustal-scale geometry shown on Fig. 9. The shear strain (γ) is accessed using the angle (α) between S and C planes from the equation: $\gamma = 2\cot g\ (\alpha)$ (Ramsay and Graham, 1970). All measurements of α angle were performed on sections cut perpendicular to the foliation and parallel to the WNW-ESE-trending lineation. The measurement error is $\pm 2^\circ$, corresponding to the local variation in the foliation strike. The theoretical displacement (D, in kilometres) along the shear zone is derived from the shear strain and the thickness of shear zone (L, in kilometres) from the equation: $D = \int_L \gamma\, dx$ (Ramsay and Graham, 1970).

On thin sections, average α angles increase eastward from 20° to 55°. The corresponding shear strain γ increases eastward from 3.0 to 3.1. The thickness L of strong (5.5 km), moderate (2.5 km), and weak strain zones (2 km) of the AF is obtained graphically using the cross-section geometry on Fig. 8B. The computed displacement D across individual strain zone decreases eastward, from 16.7 km for orthogneisses, to 6.1 km for mica-schists, and 6.2 km for granites-migmatites. Accordingly, a net slip of $\sim$29 km is derived for the normal-dextral movement along the whole AF. At crustal scale, the α angle of 31° is constant though a 10-km-thick strain zone, providing a shear strain of $\gamma = 2.88$. These two estimates agree with those obtained graphically on crustal-scale cross-sections ($D = 30$ km) and those obtained using the metamorphic break on both sides of the AF (26 km; Bellot, 2001).

7. Discussion

7.1. Timing of doming versus timing of melting

According to foliation and lineation pattern, microstructures, and seismic data, the footwall of the Argentat fault has experienced coeval normal-dextral shearing and doming at a crustal scale. The syntectonic hydrothermal activity along the AF is related to the 337–335 Ma interval (Roig et al., 2002). Clastic sedimentation along the active AF took place around 332 Ma (Bruguier et al., 1998). Our structural and microstructural data show that leucogranites dykes and sills (328–319 Ma) and granodiorite plutons (not dated) were deformed by normal-dextral shearing along the AF during and after their emplacement. Doming ended before dextral shearing began along the Pradines fault ($\sim$315 Ma). Accordingly, normal-dextral shearing along the AF, doming and granite emplacement in the Millevaches dome are both likely related to the same 337–315 Ma interval.

The extensional shear zone flanking the Millevaches dome to the east may be (1) an early shear zone that was abandoned during horizontal dome growth (e.g. Brun and Van Den Driessche, 1994; Brun et al., 1994; Gautier and Brun, 1994; Gautier et al., 1999), (2) the edge of the main normal shear zone, (3) an intra-dome shear zone that accommodates extension within the dome. The crustal-scale geometry of the granite Millevaches (Fig. 10) favours the hypothesis of the abandonment of an early detachment. This may occur after doming (more rapid than shearing) that likely result from addition of important volume of melt within the footwall and subsequent density decrease and horizontal

dome growth. Abandonment of the early detachment is effective when a new shear zone breaks through the initial deformation zone.

7.2. Timing of melt emplacement within the Millevaches dome

Geometrical relationships, kinematic analysis and radiometric dating indicate that three main stages of melt emplacement occurred within the Millevaches dome (Fig. 11).

During Early Carboniferous continental collision (355–345 Ma), calk-alkaline magmatism affected the entire region during crustal-scale transpression (Fig. 11A) (Roig et al., 1996, 1998). Scarce monzogranites (Fig. 4A) intruded the Millevaches dome. In the Limousin units, at the same time, sheeted-dykes complexes of granodiorite were emplaced along the active sinistral Estivaux shear zone (346 ± 3.5 Ma, biotite ^{40}Ar-^{39}Ar dating; Roig et al., 1996). Also at this time, sills and dykes of granodiorite were emplaced in the hinge of the Tulle antiform (Fig. 2B) (354 ± 9 Ma and 350 ± 8 Ma, biotite ^{40}Ar-^{39}Ar dating; Roig, 1997).

During early stages of Middle Carboniferous synorogenic extension (335–330 Ma), abundant leucogranites and granodiorites intruded the Millevaches dome (Fig. 11B). Fabric patterns, which reflect interference between emplacement of plutons and the regional extensional strain field (Brun and Pons, 1981), indicate contrasting modes of granite emplacement along the active AF. Leucogranites in the western part of the dome emplaced as meter-scale dykes injected along the AF (Roig et al., 2002). Leucogranites from the dome core were emplaced by diapirism and lateral expansion along the AF. In the Limousin units, at the same time, leucogranites were emplaced as kilometre- to meter-scale sills and dykes in the hinge of the Meuzac antiform (Fig. 2B) (338–333 Ma, muscovite ^{40}Ar-^{39}Ar dating; Alexandrov, 2000).

During late stages of the Middle Carboniferous synorogenic extension (~315 Ma), scarce leucogranites ascended along the Pradines dextral shear zone and expanded laterally (Fig. 11C). In the Limousin units, at the same time, leucogranites (317 ± 3 Ma; monazite U-Pb age; Lafon, 1986) were emplaced in an antiformal refold of the hinge of the St. Germain-les-Belles synform (Fig. 2B). A crustal-scale tectonic scenario considering this sequence of melt emplacement and the development of the strain pattern is discussed below.

7.3. A kinematic model for the Millevaches dome

Magma emplacement within the whole region, including the Millevaches dome, predated normal shearing on the AF and began during collision. However, the main stage of granite intrusion within the Millevaches dome was coeval with normal-dextral shearing along the AF during synorogenic extension. Exhumation of deep-seated rocks, partial melting, and low-pressure metamorphism also occurred during leucogranite emplacement within the dome. These relationships point out the key role of Variscan synorogenic extension in the development of the Millevaches dome. The dome is interpreted to be a crustal-scale extensional gneiss dome formed during crustal-scale progressive shearing (Fig. 12). Because of the transition from magmatic to solid-state deformation widely observed in the plutons within the dome (Floc'h, 1983; Feix, 1988; Roig et al., 2002), it is assumed that Argentat normal shearing along the AF and coeval Millevaches doming took place during melt emplacement and until melt solidification. The presented model displays a range of similarity with that of Johnson (2006) that suggests the rooting of extensional shear zones of the Shuswap metamorphic core complex within mid-crustal granitic melts. It is fairly in agreement with the model of Lister and Baldwin (1993) that proposes that the formation of metamorphic core complexes may be triggered by plutonic

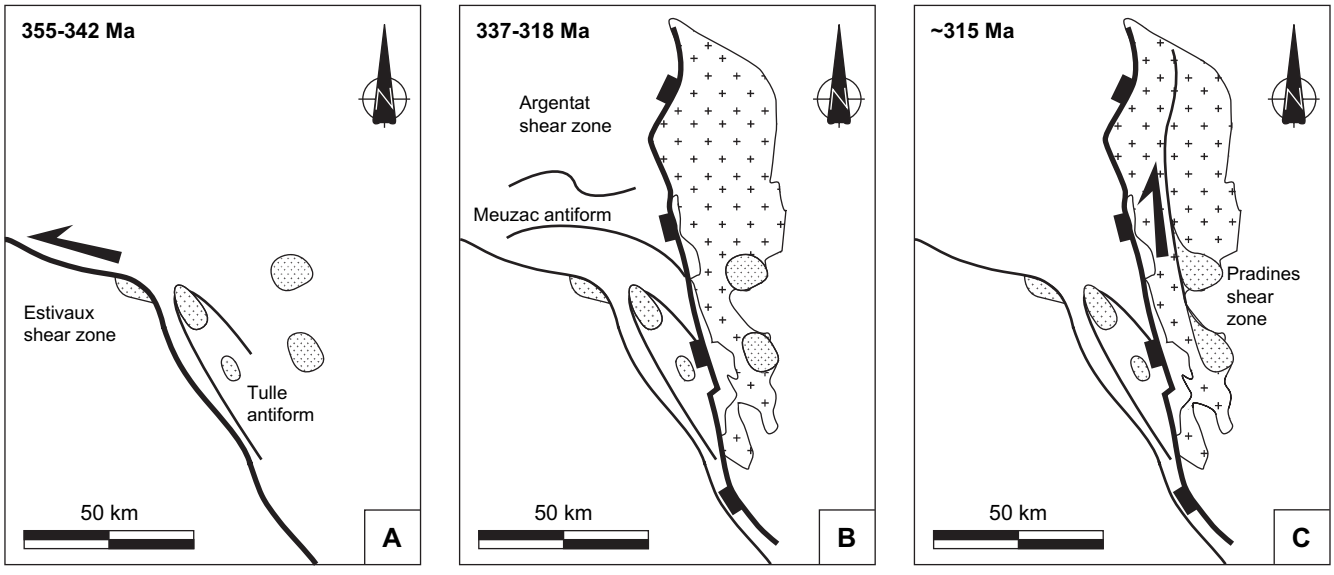

Fig. 11. Ultra-simplified maps showing the sequence of granite emplacement within the Limousin units and the Millevaches dome. (A) Collision-related granite. (B) Extension-related granite. (C) Transtension-related granite.

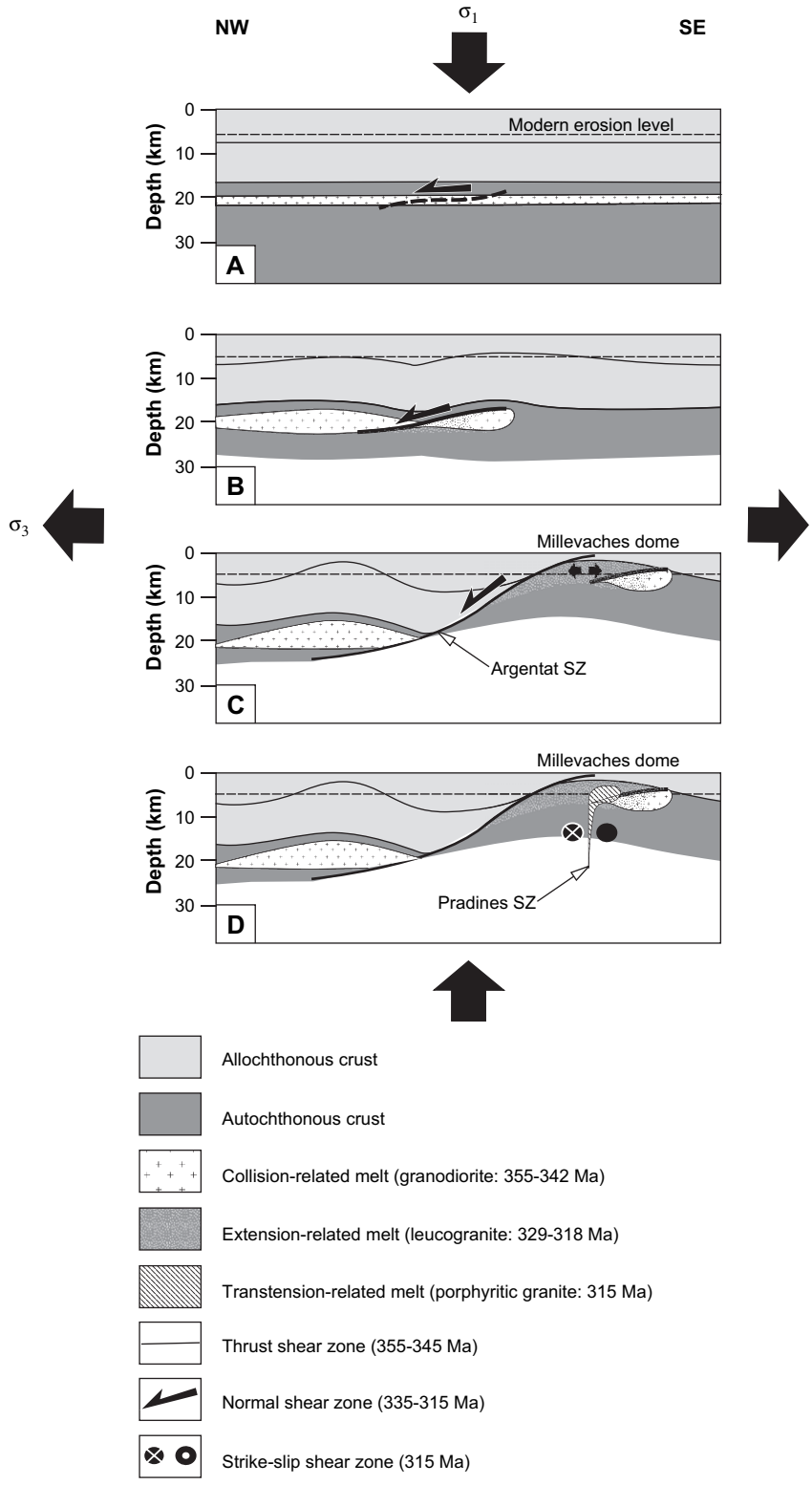

Fig. 12. A three-stage kinematics model explaining nucleation and growth of the Millevaches dome in relation to the Variscan synorogenic extension. (A) Pre-extension stage (344–342 Ma): vertical partitioning of the crust inherited from collision and introduction of a mid-crustal weak layer. (B) Dome nucleation stage (337–334 Ma): shearing dominates on plutonism. Partial melting of the fertile rocks. (C) Dome growth stage (329–318 Ma): plutonism dominates on shearing. (D) Latest stage (~315 Ma): scarce granite emplacement and shear deformation along the strike-slip Pradines fault.

activity in the middle crust during episodes of continental extension. However, the presented model points to the respective role of pre-extension and syn-extension melts in the development of extensional domes. Based on these assessments, a three-stage kinematic model is proposed below (Fig. 12).

During a pre-extension stage (344–342 Ma), collisional tectonics and monzogranitic magmatism led to melt production and accumulation at the roof of the Parautochthonous Units to form a thin (~2-km-thick) molten zone (Fig. 12A) (Bellot, 2001). Melt emplacement produced high temperature metamorphism at intermediate pressure in the host-rock. Incompletely solidified plutons within the same crustal level represent rheological heterogeneities that may induce strain localization and therefore favour nucleation of shear zones (e.g. Neves et al., 1996).

During the nucleation stage (337–334 Ma), WNW-ESE-trending horizontal extension led to partial melting (Be Mézème, 2005) at the roof of the Parautochthonous Units (Bellot, 2001) and stretching of cooling plutons (Fig. 12B). Deformation likely first concentrated within the plutons, leading to nucleation of a normal shear zone. The early low dip of the shear zone is favoured by (1) horizontal partitioning of the crust involved (Hanmer et al., 1996), (2) the weak rheology of the rock involved in shear deformation. The low-angle shear zone may have developed during a short time span and under very reduced stress (Gueydan et al., 2003). Normal slip along the shear zone initiated the processes of exhumation and partial melting, as well as the syntectonic emplacement of leucogranites in the footwall near the AF. Normal simple shear applied on incompletely solidified plutons is the main processes for dome nucleation.

During the growth stage (329–318 Ma), the crustal extensional strain field is accommodated by growth of the AF that flattens both at the top and at the base of the molten layer (Fig. 12C). Normal slip along the AF led to progressive exhumation in the footwall. Exhumation favours partial melting of the fertile rocks and ongoing production of syntectonic melt. As the solid phase component of melts increased, the crystal mush began to behave as a solid, and the shear zone propagated into the country rocks. Horizontal stretching of the footwall hinge favours production of large amounts of leucogranite within the dome. Their emplacement led to upwarping of the footwall, and to decrease of the footwall density relative to the hangingwall density. Diapirism itself likely led to progressive tilting of the footwall and to increase the dip of the AF. Addition of a large quantity of melt likely favours more efficient exhumation than that produced by normal shearing slip only. The resulting structures are the asymmetric Millevaches dome in the footwall, a symmetric dome of melt in the middle crustal levels of the hangingwall, and upright folds in the upper crustal levels of the hangingwall (Fig. 10). The emplacement of the leucogranites in a relatively cold basement led to high temperature metamorphism of the host-rock, and to discharge hydrothermal fluids (Floc'h, 1983). Channelling of fluids along the AF led to fluid–rock interactions and subsequent hydrothermal alteration and low temperature metamorphism in the host-rock. Significant addition of melt on the one hand, and resulting diapirism on the other hand are the main processes for dome growth during horizontal extension.

During the late stage, extension is accommodated by ductile strike-slip shearing along the Pradines fault along which a few leucogranites have intruded and previous granites are deformed (Fig. 12D).

8. Conclusion

Pre- and syn-extension melt-assisted nucleation and growth of extensional gneiss domes and the adjacent detachment fault are inferred therein, based on the example of the Palaeozoic Millevaches dome and the Argentat fault. The gneiss dome nucleates in response to crustal-scale, horizontal extension within a mid-crustal layer of collision-related melts. Progressive dome growth is controlled by competition between normal shearing, due to crustal extension, and diapirism, due to addition of melt within the dome. During early extensional deformation, shearing dominates and leads to create low-angle shear zones within the molten layer. Later, following addition of a large quantity of melt, diapirism dominates and leads to steepening of the shear zone. The resulting structure is a strongly asymmetric extensional dome. Pre-extension and syn-extension melts, by their amount, structure, and location, play a key role at all stages of the development of extensional gneiss domes.

Acknowledgments

This work has been supported by the BRGM (3D Mapping and Metallogeny of the French Massif Central Project). This paper is also a contribution to the GeoFrance3D program. I thank Steve Marshak and an anonymous reviewer for their constructive reviews and detailed comments that help to improve the quality of the paper. I also thank Dave Vanko for final improvements of the quality of the English.

References

Arnaud, F., Boullier, A.M., Burg, J.P., 2004. Shear structures and microstructures in micaschists: the Variscan Cevennes duplex (French Massif Central). Journal of Structural Geology 26, 855–868.

Alexandrov, P., 2000. Géochronologie U/Pb et $^{40}Ar/^{39}Ar$ de deux segments de la chaîne varisque: le haut limousin et les Pyrénées orientales. PhD thesis, INPL Nancy, France, 186 pp.

Bellot, J.-P., 2001. La structure de la croûte varisque du Sud-Limousin (Massif central français) et ses relations avec les minéralisations aurifères tardi-orogéniques: apport des données géologiques, gitologiques, géophysiques et de la modélisation 3D. PhD thesis, Université de Monpellier, France, 309 pp.

Bellot, J.-P., 2004. Shear zone-hosted polymetallic sulphides in the South Limousin area, Massif Central, France: Remobilized sulphide deposits related to Variscan collisional tectonics and amphibolite facies metamorphism. Economic Geology 99, 819–827.

Bellot, J.-P., Roig, J.-Y., Genna, A., 2005. The Hospital coal basin (Massif Central, France): relay of the left-lateral strike-slip Argentat fault in relation to the Variscan postorogenic extension. Bulletin de la Société Géologique de France 177, 141–149.

Be Mézème, E., 2005. Contribution de la géochronologie U-Th-Pb sur monazite à la compréhension de la fusion crustale dans la chaîne varisque

française et implication géodynamique. PhD thesis, Université d'Orléans, France, 277 pp.

Bitri, A., Truffert, C., Bellot, J.-P., Bouchot, V., Milési, J.P., Ledru, P., Roig, J.Y., 1999. Imagerie des paléochamps hydrothermaux As-Au-Sb d'échelle crustale et des pièges associés dans la chaîne varisque: sismique réflexion verticale (GéoFrance 3D: Massif Central français). Paris, Comptes Rendus de l'Académie des Sciences 329, 771–777.

Bouchez, J.L., Jover, O., 1986. Le Massif Central: un chevauchement de type himalayen vers l'ouest-nord-ouest. Paris, Comptes Rendus de l'Académie des Sciences 302, 675–680.

Brown, M., 1993. The definition of metatexis, diatexis and migmatite. Proceedings of the Geological Association 84, 371–382.

Bruguier, O., Becq-Giraudon, J.-F., Bosch, D., Lancelot, J., 1998. Late Visean (Upper Mississipian) hidden basin in the internal zones of the Variscan belt: U-Pb zircon evidence from the French Massif Central. Geology 26, 627–630.

Brun, J.P., Pons, J., 1981. Patterns of interference between granite diapirism and regional deformation (abstract). Journal of Structural Geology 3, 93.

Brun, J.P., Burg, J.P., 1982. Combined thrusting and wrenching in the Ibero-Armorican arc: a corner effect during continental collision. Earth and Planetary Science Letters 6, 319–332.

Brun, J.P., Van Den Driessche, J., 1994. Extensional gneiss domes and detachment fault system: structure and kinematics. Bulletin de la Société Géologique de France 165, 519–530.

Brun, J.P., Sokoutis, D., Van Den Driessche, J., 1994. Analogue modelling of detachment fault systems and core complexes. Geology 22, 319–322.

Buck, R., 1991. Modes of continental lithospheric extension. Journal of Geophysical Research 96, 10275–10286.

Burg, J.P., Brunel, M., Gapais, D., Chen, G.M., Liu, G.H., 1984. Deformation of leucogranites of the crystalline main central thrust sheet in southern Tibet (China). Journal of Structural Geology 6, 535–542.

Burg, J.P., Van Dendrissche, J., Brun, J.P., 1994. Syn- to post-thickening extension in the Variscan Belt of Western Europe: Modes and structural consequences. Géologie de la France 3, 33–51.

Coney, P.J., Harms, T.A., 1984. Cordilleran metamorphic core complexes: Cenozoic extensional relics of Mesozoic compression. Geology 12, 550–554.

Crittenden, M.D., Coney, P.J., Davis, G.H., 1980. Cordilleran Metamorphic Core Complexes. Geological Society of America Memoir, Boulder, CO, pp. 490.

Dèzes, P.J., Vannay, J.-C., Steck, A., Bussy, F., Cosca, M., 1999. Synorogenic extension: quantitative constraints on the age and displacement of the Zanskar shear zone (northwest Himalaya). Geological Society of America Bulletin 111, 364–374.

Echtler, H., Malavieille, J., 1990. Extensional tectonics, basement uplift and Stephano-Permian collapse basin in a late Variscan metamorphic core complex (Montagne Noire, Southern Massif Central). Tectonophysics 177, 125–138.

Faure, M., Monié, P., Pin, C., Maluski, H., Leloix, C., 2002. Late Visean thermal event in the northern part of the French Massif Central: new $^{40}Ar/^{39}Ar$ and Rb-Sr isotopic constraints on the Hercynian syn-orogenic extension. International Journal of Earth Sciences 91, 53–75.

Faure, M., 1995. Late carboniferous extension in the Variscan French Massif Central: Tectonics 14, 132–153.

Feix, I., 1988. Etude géologique dans le Sud-Millevaches: lithologie, géochimie, métamorphisme et structure des séries métamorphiques situées au Sud de la Vallée de la Dordogne. Place dans le Massif central français occidental. Unpublished thesis, Université d'Orléans, France, 535 pp.

Floc'h, J.P., 1983. La série métamorphique du Limousin central: une traverse de la branche ligérienne de l'orogène varisque, de l'Aquitaine à la zone broyée d'Argentat (Massif central français). Unpublished thesis, Université de Limoges, France, 450 pp.

Franke, W., 2000. The mid-European segment of the Variscides: tectonostratigraphic units, terrane boundaries and plate tectonic evolution. Geological Society of London Special Publication, vol. 179, pp. 35–61.

Gautier, P., Brun, J.-P., 1994. Crustal-scale geometry and kinematics of late-orogenic extension in the central Aegean (Cyclades and Ewia Island). Tectonophysics 238, 399–424.

Gautier, P., Brun, J.P., Moriceau, R., Sokoutis, D., Martinod, J., Jolivet, L., 1999. Timing, kinematics and cause of Aegean extension; a scenario based on a comparison with simple analogue experiments. Tectonophysics 315, 31–72.

Gébelin, A., 2004. Déformation et mise en place des granites (360–300 Ma) dans un segment de la Chaîne Varisque (Plateau de Millevaches, Massif Central). Unpublished PhD thesis, Université Monpellier II, France, 234 pp.

Gébelin, A., Martelet, G., Chen, Y., Brunel, M., Faure, M., 2006. Structure of late Variscan Millevaches leucogranite massif in the French Massif Central: AMS and gravity modelling results. Journal of Structural Geology 28, 148–169.

Gueydan, F., Leroy, Y.M., Jolivet, L., Agard, P., 2003. Analysis of continental localization induced by reaction-softening and microfracturing. Journal of Geophysical Research 108 (B2), doi:10.1029/2001JB000611.

Guillot, P.L., 1981. La série métamorphique du Bas-Limousin: de la vallée de l'Isle à la vallée de la Vézère, le socle en bordure du bassin aquitain. Unpublished thesis, Université d'Orléans, France, 391 pp.

Guillot, S., Hodges, K.V., Lefort, J.P., Pêcher, A., 1994. New constrains on the age of the Manaslu leucogranite: evidence for episodic tectonic denudation in the central Himalayas. Geology 22, 559–562.

Hanmer, S., Corrigan, D., Ganas, A., 1996. Orientation of nucleating faults in anisotropic media: insights from three-dimensional deformation experiments. Tectonophysics 267, 275–290.

Johnson, B.J., 2006. Extensional shear zones, granitic melts, and linkage of overstepping normal faults bounding the Shuswap metamorphic core complex, British Columbia. GSA Bulletin 118, 366–382.

Labernardière, H., Lefavrais-Raymond, A., Astruc, J.G., MONIER, G., 1992. Carte géologique de la France (1/50 000), feuille Argentat (786). – BRGM, Orléans. Notice explicative par Labernardière H., Lefavrais-Raymond A. et Astruc J.-G., 66 p.

Lafon, J.M., 1986. Géochronologie U-Pb appliquée à deux segments du Massif central français: le Rouergue oriental et le Limousin central. PhD thesis, Université Montpellier II, France, 152 pp.

Lardeaux, J.M., Ledru, P., Daniel, I., Duchène, S., 2001. The Variscan French Massif central – a new addition to the ultra-high pressure metamorphic 'club': exhumation processes and geodynamic consequences. Tectonophysics 332, 143–168.

Ledru, P., Costa S., Echler, H., 1994. Structure. In: Keppie, J.D. (Ed.), Pre-Mesozoic Geology in France and Related Areas. Part III, The Massif Central: Springer-Verlag, Berlin Heidelberg, pp. 305–323.

Ledru, P., Courrioux, G., Dallain, C., Lardeaux, J.M., Montel, J.M., Vanderhaeghe, O., Vitel, G., 2001. The Velay dome (French Massif Central): melt generation and granite emplacement during orogenic evolution. Tectonophysics 342, 207–237.

Lister, G.S., Baldwin, S.L., 1993. Plutonism and the origin of metamorphic core complexes. Geology 21, 607–610.

Malavieille, J., 1993. Late orogenic extension in mountains belts: insights from the Basin and Range and the Late Paleozoic Variscan belt. Tectonics 12, 1115–1130.

Malavieille, J., Guilhot, S., Costa, S., Lardeaux, J.M., Gardien, V., 1990. Collapse of the thickened Variscan crust in the French Massif Central: Mont du Pilat extensional shear zone and St.-Etienne carboniferous basin. Tectonophysics 177, 139–149.

Mattauer, M., Brunel, M., Matte, P., 1988. Failles normales ductiles et grands chevauchements. Une nouvelle analogie entre l'Himalaya et la chaîne hercynienne du Massif Central français. Paris, Comptes Rendus de l'Académie des Sciences 306, 671–676.

Matte, P., 2001. The Variscan collage and orogeny (480–290 Ma) and the tectonic definition of the Armorica microplate: a review. Terra Nova 13, 117–121.

McClelland, W.C., Gilotti, J.A., 2003. Late-stage extensional exhumation of high-pressure granulites in the Greenland Caledonides. Geology 31, 259–262.

Mezure, J.F., 1981. Orientation préférentielle des mégacristaux de feldspath potassique dans les granites. Application à l'étude structurale des granites d'Egletons et de Meymac (Corrèze, Massif central français). Bulletin de la Société Géologique de France 7, 641–649.

Monier, G., 1980. Pétrologie des granitoïdes du Sud-Millevaches (Massif central français). Minéralogie, géochimie, géochronologie. Doctorate thesis, Université de Clermont-Ferrand, France, 288 pp.

Mouret, G., 1922. Sur le prolongement de la fracture d'Argentat (Corrèze) dans la région du Dorat (Haute-Vienne). Paris, Comptes Rendus de l'Académie des Sciences 174, 553.

Mouthier, B., 1976. Lithostratigraphie et métamorphisme des formations cristallophylliennes de la région de Chateauneuf-la-forêt (Haut Limousin, Massif central français). Thesis, Université Lyon I 508, 161 pp.

Neves, S.P., Vauchez, A., Archanjo, C.J., 1996. Shear-zone controlled magma emplacement or magma-assisted nucleation of shear zones? Insights from northeast Brazil. Tectonophysics 262, 349–364.

Ramsay, J.G., Graham, R.H., 1970. Strain variations in shear belts. Canadian Journal of Earth Sciences 7, 786–813.

Roig, J.Y., 1997. Evolution tectono-métamorphique d'un segment de la chaîne hercynienne. Rôle du plutonisme dans la caractérisation des tectoniques du Sud-Limousin (Massif central français). Ph. D. Thesis, Université d'Orléans, France, 287 p.

Roig, J.Y., Faure, M., 2000. La tectonique cisaillante polyphasée du Sud-Limousin (Massif Central français) et son interprétation dans un modèle d'évolution polycyclique de la chaîne hercynienne. Bulletin de la Société géologique de France 171, 295–307.

Roig, J.Y., Faure, M., Ledru, P., 1996. Polyphase wrench tectonics in the southern French Massif Central: kinematic inferences from pre- and syntectonic granitoids. Geologische Rundschau 85, 138–153.

Roig, J.Y., Faure, M., Maluski, H., 2002. Superimposed tectonic and hydrothermal events during the late-orogenic extension in the Western French Massif central: a structural and $^{40}Ar/^{39}Ar$ study. Terra Nova 14, 25–32.

Roig, J.Y., Faure, M., Truffert, C., 1998. Folding and granite emplacement inferred from structural, strain, TEM, and gravimetric analyses: The case study of the Tulle antiform, SW French Massif Central. Journal of Structural Geology 20, 1169–1189.

Smith, B., Reynolds, S.J., Day, H.W., Bodnar, R.J., 1991. Deep-seated fluid involvement in brittle-ductile deformation and mineralization, South Mountains metamorphic core complex, Arizona. Geological Society of America Bulletin 103, 559–569.

Spear, F.S., Kohn, M.J., Cheney, J.T., 1999. P-T paths from anatectic pelites. Contribution to Mineralogy and Petrology 134, 17–32.

Thompson, A.B., Connolly, J.A.D., 1995. Melting of the continental crust: some thermal and petrological constraints on anatexis in continental collision zones and other tectonic settings. Journal of Geophysical Research 100, 15565–15579.

Thompson, A.B., Ridley, J.R., 1987. Pressure-temperature-time (P-T-t) histories of orogenic belts. Philosophical Transaction of the Royal Society, London A321, 27–45.

Vanderhaeghe, O., Teyssier, C., 2001. Partial melting and flow of orogens. Tectonophysics 342, 451–472.

Vanderhaeghe, O., McDougall, I., Dunlap, W.J., Teyssier, C., 2003. Cooling and exhumation of the Shuswap metamorphic core complex constrained by $^{40}Ar/^{39}Ar$ thermochronology. Geological Society American Bulletin 115, 200–216.

Wernicke, B., Axen, G.J., 1988. On the role of isostasy in the evolution of normal fault systems. Geology 16, 848–851.

Ziegler, P., 1989. Evolution of Laurussia. Kluwer Academic Publishers, Dordrecht, Boston, London, 102 pp.